PHYSICAL REVIEW D **87,** 114020 (2013)

Ghost propagator and ghost-gluon vertex from Schwinger-Dyson equations

A. C. Aguilar,[1] D. Ibáñez,[2] and J. Papavassiliou[2]

[1]*Institute of Physics "Gleb Wataghin", University of Campinas-UNICAMP, 13083-859 Campinas, São Paulo, Brazil*
[2]*Department of Theoretical Physics and IFIC, University of Valencia and CSIC, E-46100 Valencia, Spain*

(Received 14 March 2013; published 27 June 2013)

We study an approximate version of the Schwinger-Dyson equation that controls the nonperturbative behavior of the ghost-gluon vertex in the Landau gauge. In particular, we focus on the form factor that enters in the dynamical equation for the ghost dressing function, in the same gauge, and derive its integral equation, in the "one-loop dressed" approximation. We consider two special kinematic configurations, which simplify the momentum dependence of the unknown quantity; in particular, we study the soft gluon case and the well-known Taylor limit. When coupled with the Schwinger-Dyson equation of the ghost dressing function, the contribution of this form factor provides considerable support to the relevant integral kernel. As a consequence, the solution of this coupled system of integral equations furnishes a ghost dressing function that reproduces the standard lattice results rather accurately, without the need to artificially increase the value of the gauge coupling.

DOI: 10.1103/PhysRevD.87.114020 PACS numbers: 12.38.Aw, 12.38.Lg, 14.70.Dj

I. INTRODUCTION

One of the few nonperturbative frameworks available for the study of the infrared sector of QCD in the continuum are the Schwinger-Dyson equations (SDEs), which govern the dynamics of the basic Green's functions of the theory [1–4]. Despite the well-known limitations intrinsic to this formalism, a variety of theoretical and technical advances has provided new valuable insights on some of the most fundamental nonperturbative phenomena of QCD, such as quark confinement, dynamical mass generation, and chiral symmetry breaking [3,5–8]. Particularly important in this ongoing effort is the systematic confrontation of the SDE predictions with the results of large-volume lattice simulations [9–14], leading not only to quantitative refinements but, in some cases, to critical revisions of the underlying physical concepts [7,15–17].

The quantitative understanding of the ghost sector of QCD constitutes a long-standing challenge for the SDE practitioners. Without a doubt, the most fundamental quantity in this context is the ghost propagator, $D(p^2)$ and the corresponding dressing function, $F(p^2) = p^2 D(p^2)$; in fact, the infrared behavior of the latter, in the Landau gauge (LG), has been traditionally associated with a particular realization of color confinement [18–21].

In recent years, various lattice studies, both in $SU(2)$ and $SU(3)$, together with numerous analytic approaches, find a massless ghost propagator with an infrared finite dressing function [7,9,11,17,22]. In addition, in the same gauge, the gluon propagator obtained on the lattice is finite in the deep infrared, supporting the notion of an effectively massive gluon [23–25]. In fact, the dynamical gluon mass generation, first proposed in Ref. [26] and further developed in a number of recent works, provides a unified explanation for the observed finiteness of both aforementioned quantities [7,27–30]. Specifically, an infrared finite $F(p^2)$ emerges as a direct consequence of the massiveness of the gluon propagator; such a gluon propagator, when inserted in the SDE of the ghost propagator, saturates the logarithms associated with the $F(p^2)$, thus making it finite at the origin.

However, what has been more difficult to obtain from a self-consistent SDE analysis is the entire shape and size of $F(p^2)$ provided by the lattice [7,31,32]. In fact, even when one substitutes into the ghost SDE the gluon propagator furnished by the lattice, but keeping the ghost-gluon vertex at its tree-level value, the resulting $F(p^2)$ is significantly suppressed compared to that of the lattice [7]; to reproduce the lattice result, one has to artificially increase the value of the gauge coupling from the correct value $\alpha_s = 0.22$ to $\alpha_s = 0.29$ [33].

It would seem, therefore, that the main reason for the observed discrepancy ought to be traced back to the way in which the fully dressed ghost-gluon vertex, Γ_ν, appearing in the ghost SDE, is approximated. Even though preliminary lattice studies indicate that the deviations of Γ_ν from its tree-level value are relatively moderate [34–38], the highly nonlinear nature of the ghost SDE may lead to considerable enhancements. In fact, a modest increase of the relevant vertex form factor in the region of momenta that provides the largest support to the ghost SDE may account for the bulk of the required effect.

The purpose of this article is to obtain the nonperturbative behavior of this important missing ingredient, using as a starting point the integral equation that controls its momentum evolution. Specifically, we will determine the relevant vertex form factor from an approximate version of the SDE satisfied by the vertex Γ_ν itself, in the LG. To be sure, the vertex SDE has a complicated skeleton expansion, involving various unknown (or only partially known) quantities, such as multiparticle kernels. The basic approximations we employ at the level of the vertex SDE are the

following. (i) We consider only the first two diagrams in this expansion; this corresponds to the "one-loop dressed" truncation [39]. (ii) Inside these diagrams, we replace full vertices by their tree-level values but keep *fully dressed* ghost and gluon propagators. (iii) For the numerical analysis of the resulting integrals, we use as input for the full gluon propagators the lattice data of Refs. [11,12].

From the conceptual point of view, the general procedure outlined above relies crucially on the constructive interplay between the SDEs and lattice, which has been rather fruitful in recent years [40]. Specifically, it is clear that, whereas in their original form the SDEs are obtained directly from the path integral of the theory (and are, in that sense, exact), the practical need to carry out simplifications and truncations converts this approach into an approximate method. Part of the inherent difficulty in dealing with these coupled nonlinear equations may be reduced by employing lattice results for some of the Green's functions appearing inside them. A particular example where this strategy turned out to be rather effective has been the study of chiral symmetry breaking [8]. In particular, whereas the pure SDE treatment (after unavoidable approximations) fails to furnish to the kernel of the quark gap equation the support necessary for triggering the aforementioned phenomenon, replacing the SDE gluon propagator by its lattice counterpart provides a considerable enhancement. The synergy is completed by noting that the final portion of missing strength is furnished by the SDEs themselves, namely, the one-loop dressed approximation of the quark-gluon vertex, through a treatment not too dissimilar to the one followed here.

After these general comments, let us return to the task at hand. The tensorial decomposition of Γ_ν consists of two form factors [see Eq. (2.2)]; however, given that this vertex will be inserted in the ghost SDE, written in the LG, only the cofactor $A(-k,-p,r)$ of the ghost momentum p_ν survives. In the present study, we determine $A(-k,-p,r)$ for two particular kinematic configurations, soft gluon ($k\to 0$) and soft ghost ($p\to 0$), thus converting it, in both cases, to a function of a single momentum only, $A(0,-p,p)$ and $A(-k,0,k)$, respectively. In fact, as we will explain in detail in Sec. III, the case where $p\to 0$ is equivalent to the standard Taylor limit [41,42].

Our main results may be summarized as follows.

(i) In the soft gluon limit, the result obtained for $A(0,-p,p)$ displays a moderate peak around 1 GeV, corresponding to a 20% increase with respect to the tree-level value; this result compares rather well with the existing lattice data [36,37]. As we will explain in detail in Sec. IV A, this particular kinematic configuration is not relevant for the ghost SDE; however, it serves as a preliminary test of the overall faithfulness of the approximations employed.

(ii) The numerical solutions for the coupled system of integral equations determining $F(p^2)$ and $A(-k,0,k)$ give rise to a ghost dressing function that is in excellent agreement with the lattice data [11,12]. The corresponding solution for $A(-k,0,k)$ is characterized by a rather pronounced maximum, centered again around 1 GeV, reaching a value of about 1.5. In this analysis we use $\alpha_s = 0.22$, which corresponds to the momentum-subtraction (MOM) value for the point $\mu = 4.3$ GeV [43], used to renormalize the gluon propagator obtained from the lattice.

The article is organized as follows. In Sec. II we introduce the necessary notation and set up the SDE for the ghost dressing function, paying particular attention to the way that the fully dressed ghost-gluon vertex enters in it. In Sec. III we carry out the analysis at the level of the SDE of the ghost-gluon vertex and derive the corresponding closed expressions in the two kinematic limits of interest. In Sec. IV we present the numerical treatment of the equations derived in the previous sections. In particular, we first compute the case of the soft gluon, and then we proceed to the solution of the coupled system. Finally, our conclusions and discussion are presented in Sec. V.

II. GHOST DRESSING FUNCTION AND THE GHOST-GLUON VERTEX

In this section we introduce the SDE for the ghost propagator in the LG and discuss some of its basic properties and features. Of particular interest is the dependence of this equation on the surviving component of the ghost-gluon vertex and the numerical implications of approximating it by its tree-level value. Let us warn the reader at this point that, whereas the analysis of the present section will be carried out in Minkowski space, in subsequent sections the Euclidean version of the corresponding equations will be also employed; the rules for implementing this conversion are given in Eq. (3.10).

Our starting point is the full ghost-gluon vertex, shown in Fig. 1 and denoted by

$$\Gamma_\nu^{nbc}(-k,-p,r) = g f^{nbc}\Gamma_\nu(-k,-p,r), \quad r = k+p, \tag{2.1}$$

with k representing the momentum of the gluon and p of the antighost. The most general tensorial structure of this vertex is given by

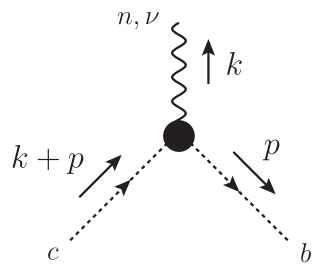

FIG. 1. The fully dressed ghost-gluon vertex.

$$\Gamma_\nu(-k,-p,r) = A(-k,-p,r)p_\nu + B(-k,-p,r)k_\nu; \quad (2.2)$$

at tree-level, the two form factors assume the values $A^{[0]}(-k,-p,r) = 1$ and $B^{[0]}(-k,-p,r) = 0$, giving rise to the bare ghost-gluon vertex $\Gamma^{[0]}_\nu = p_\nu$.

The form factors A and B may be formally projected out by contracting Γ_ν with the vectors

$$\varepsilon^A_\nu(k,p) = \frac{k^2 p_\nu - (k\cdot p)k_\nu}{k^2p^2 - (k\cdot p)^2}, \qquad \varepsilon^B_\nu(k,p) = \frac{p^2 k_\nu - (k\cdot p)p_\nu}{k^2p^2 - (k\cdot p)^2}, \quad (2.3)$$

namely,

$$\begin{aligned} A(-k,-p,r) &= \varepsilon^A_\nu(k,p)\Gamma^\nu(-k,-p,r), \\ B(-k,-p,r) &= \varepsilon^B_\nu(k,p)\Gamma^\nu(-k,-p,r). \end{aligned} \quad (2.4)$$

Of particular importance for the analysis that follows is the so-called "Taylor limit" of the ghost-gluon vertex, corresponding to the case of vanishing ghost momentum, $r = 0$, $p = -k$. In this special kinematic configuration, the $\Gamma_\nu(-k,-p,r)$ of Eq. (2.2) becomes

$$\Gamma_\nu(-k,k,0) = -[A(-k,k,0) - B(-k,k,0)]k_\nu. \quad (2.5)$$

Closely related to this limit is the well-known Taylor theorem, which states that, to all orders in perturbation theory,

$$A(-k,k,0) - B(-k,k,0) = 1; \quad (2.6)$$

as a result, the fully-dressed vertex assumes the tree-level value corresponding to this particular kinematic configuration, i.e., $\Gamma_\nu(-k,k,0) = -k_\nu$.

After these introductory comments, let us turn to the SDE for the ghost propagator and examine in some detail how the ghost-gluon vertex affects its structure. The relevant SDE is diagrammatically represented in the Fig. 2. Using the momenta flow and Lorentz indices as indicated in Fig. 2, the ghost SDE can be written as

$$iD^{-1}(p^2) = ip^2 - g^2 C_{\rm A}\int_k \Gamma^{[0]}_\mu(k,-k-p,p)\Delta^{\mu\nu}(k) \times \Gamma_\nu(-k,-p,k+p)D(k+p), \quad (2.7)$$

where $C_{\rm A}$ denotes the Casimir eigenvalue of the adjoint representation [N for $SU(N)$], $d = 4 - \epsilon$ is the space-time dimension, and we have introduced the integral measure

$$\int_k \equiv \frac{\mu^\epsilon}{(2\pi)^d}\int \mathrm{d}^d k, \quad (2.8)$$

with μ the 't Hooft mass. In the LG, the gluon propagator $\Delta_{\mu\nu}(q)$ has the transverse form

$$\Delta_{\mu\nu}(q) = -iP_{\mu\nu}(q)\Delta(q^2), \quad (2.9)$$

with

$$P_{\mu\nu}(q) = g_{\mu\nu} - \frac{q_\mu q_\nu}{q^2}, \quad (2.10)$$

the usual projection operator.

Clearly, due to the full transversality of $\Delta_{\mu\nu}(k)$, any reference to the form factor B disappears from the ghost SDE of Eq. (2.7). Specifically, substituting Eq. (2.2) into Eq. (2.7), we obtain

$$F^{-1}(p^2) = 1 + ig^2 C_{\rm A}\int_k \left[1 - \frac{(k\cdot p)^2}{k^2p^2}\right]A(-k,-p,k+p) \times \Delta(k)D(k+p), \quad (2.11)$$

where we have introduced the ghost dressing function, $F(q^2)$, defined as

$$D(q^2) = \frac{F(q^2)}{q^2}. \quad (2.12)$$

The renormalization of Eq. (2.11) proceeds through the replacements

$$\begin{aligned} &\Delta_R(q^2) = Z_A^{-1}\Delta(q^2), \qquad F_R(q^2) = Z_c^{-1}F(q^2), \\ &\Gamma^\nu_R(q,p,r) = Z_1\Gamma^\nu(q,p,r), \qquad g_R = Z_g^{-1}g = Z_1^{-1}Z_A^{1/2}Z_c g, \end{aligned} \quad (2.13)$$

where Z_A, Z_c, Z_1, and Z_g are the corresponding renormalization constants; the dependence of the above quantities on the renormalization point μ is suppressed. In the MOM scheme, usually employed in the SDE analysis, the renormalization conditions imposed are that, at μ, the corresponding Green's functions assume their tree-level values,

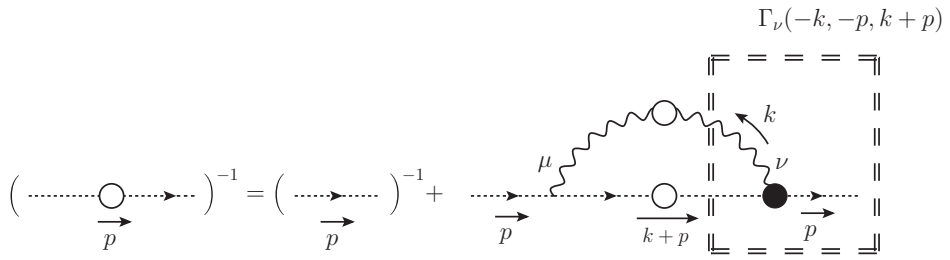

FIG. 2. The SDE for the ghost propagator given by Eq. (2.7). The white blobs represent the fully dressed gluon and ghost propagators, while the black blob denotes the dressed ghost-gluon vertex.

e.g., $\Delta_R^{-1}(q^2 = \mu^2) = \mu^2$, and $F_R(q^2 = \mu^2) = 1$ [42]. Note also that, in the LG, the form factor A is ultraviolet finite at one loop, and, therefore, no infinite renormalization constant needs to be introduced at that order for Γ^ν. In fact, one usually invokes Taylor's theorem [see Eq. (2.6)] in order to finally set $Z_1 = 1$ to all orders (see the discussion in Sec. III).

Then, the SDE becomes

$$F^{-1}(p^2) = Z_c + ig^2 C_A \int_k \left[1 - \frac{(k\cdot p)^2}{k^2 p^2}\right] A(-k, -p, k+p) \times \Delta(k) D(k+p), \tag{2.14}$$

where we have suppressed the subscript "R" to avoid notation clutter. The actual closed expression of Z_c is obtained from Eq. (2.14) itself, by imposing the aforementioned MOM renormalization condition on $F^{-1}(p^2)$.

Evidently, the explicit dependence of Eq. (2.14) on $A(-k, -p, k+p)$ requires the use of the corresponding vertex SDE, thus converting the problem of determining $F(p^2)$ into a coupled SDE system. The usual way to circumvent this technical complication has been to simply approximate $A(-k, -p, k+p)$ by its tree-level value, setting into Eq. (2.14) $A(-k, -p, k+p) = 1$.

Then, after proper renormalization along the lines discussed above and passing to the Euclidean space following the standard rules, one solves Eq. (2.14) numerically, using the lattice data of Refs. [11,12] as input for the gluon propagator. Note that this latter propagator is renormalized within the MOM scheme by imposing the standard condition $\Delta^{-1}(\mu^2) = \mu^2$ at $\mu = 4.3$ GeV, namely, the deepest available point in this set of lattice data; then, the corresponding value for $\alpha_s = g^2/4\pi$ that one should use is $\alpha_s(4.3\ \text{GeV}) = 0.22$. However, for this particular value of α_s, the solution obtained from Eq. (2.14) lies considerably below the lattice data for $F(p^2)$, as can be clearly seen from the (blue) dotted curve of Fig. 3. In order to obtain a close coincidence with the lattice, one must increase the value of $\alpha_s(4.3\ \text{GeV})$ to 0.29, thus obtaining the (red) continuous curve in Fig. 3.

It is, of course, natural to attribute the observed discrepancy to the aforementioned simple approximation employed for the ghost-gluon vertex. Therefore, to ameliorate the situation, we will determine this form factor from its corresponding SDE, in a certain kinematic limit that is relevant for the situation at hand. Specifically, given that $A(-k, -p, k+p)$ is a function of three variables, p^2, k^2, and the angle between the two (appearing in the inner product $p\cdot k$), a full SDE treatment is rather cumbersome and lies beyond our present technical powers. Instead, we will consider the behavior of $A(-k, -p, k+p)$ for vanishing p; to that end, we start out with the Taylor expansion of $A(-k, -p, k+p)$ around $p = 0$, and we only keep the first term, $A(-k, 0, k)$, thus converting A into a function of a single variable.

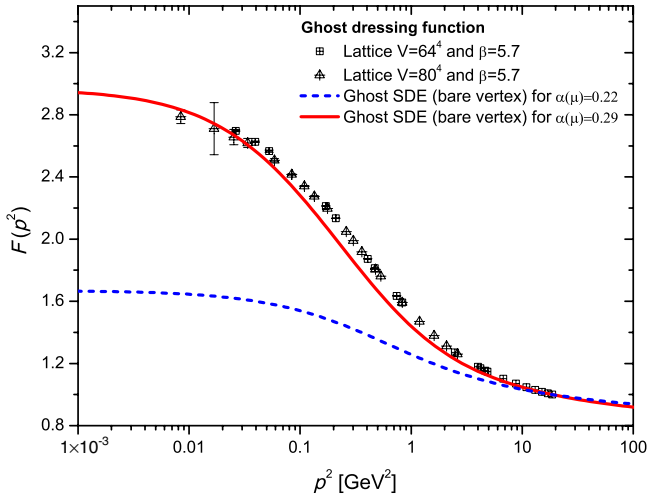

FIG. 3 (color online). Comparison of the ghost dressing function, $F(p^2)$, obtained as a solution of the ghost SDE when the ghost-gluon vertex is approximate by its bare value, with the lattice data of Refs. [11,12]. The (red) continuous curve represents the case when $\alpha_s(4.3\ \text{GeV}) = 0.29$, whereas the (blue) dashed curve is obtained when $\alpha_s(4.3\ \text{GeV}) = 0.22$.

We emphasize that the limit $p \to 0$ is taken only inside the argument of the form factor A but not in the rest of the terms appearing in the SDE of Eq. (2.14). Specifically, following the procedure explained in detail in the next section, one isolates from the ghost-gluon SDE the contribution proportional to p_ν, taking the limit $p \to 0$ in the accompanying scalar cofactor, thus arriving at a form $\Gamma_\nu(-k, -p, k+p) = p_\nu A(-k, 0, k)$. Equivalently, in terms of the projectors introduced in Eqs. (2.3) and (2.4), one has

$$A(-k, 0, k) = \lim_{p\to 0}\{\varepsilon^A_\nu(k, p)\Gamma^\nu(-k, -p, k+p)\}. \tag{2.15}$$

Thus, the approximate version of the SDE in Eq. (2.14) reads

$$F^{-1}(p^2) = Z_c + ig^2 C_A \int_k \left[1 - \frac{(k\cdot p)^2}{k^2 p^2}\right] A(-k, 0, k) \times \Delta(k) D(k+p). \tag{2.16}$$

III. GHOST-GLUON VERTEX

In this section we derive in detail the nonperturbative expression for the form factor A in two special kinematic configurations: (i) the *soft gluon limit*, in which the momentum carried by the gluon leg is zero ($k = 0$) and (ii) the *soft ghost limit*, where the momentum of the antighost leg vanishes ($p = 0$).

A. General considerations

The starting point of our analysis is the SDE satisfied by the ghost-gluon vertex, whose diagrammatic representation is shown in Fig. 4(a). One observes that the relevant

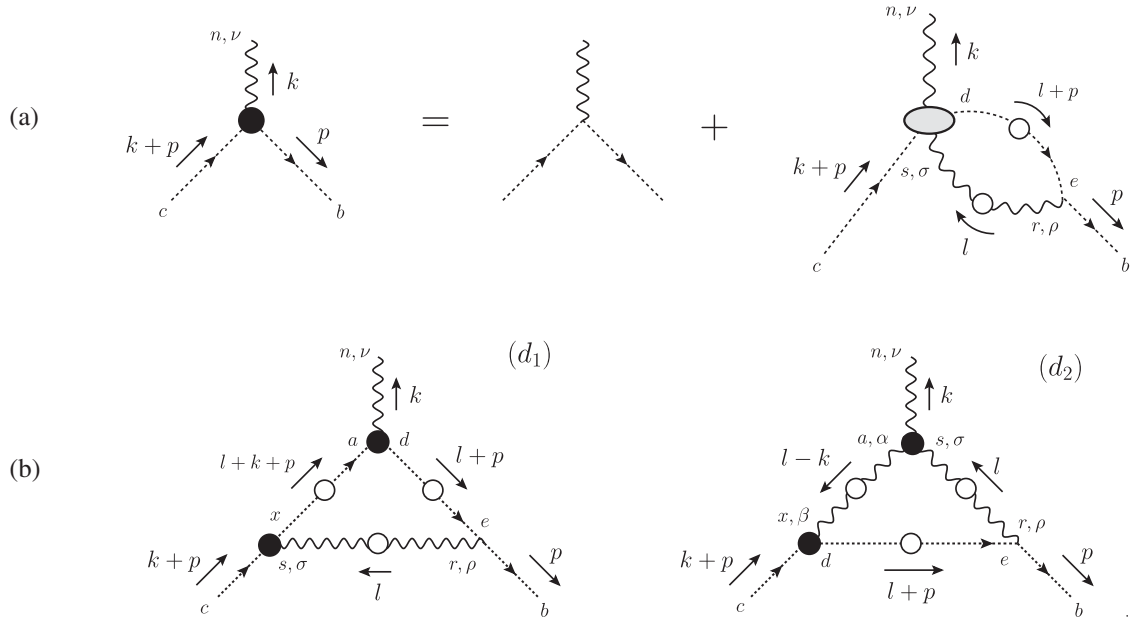

FIG. 4. (a) The complete SDE of the ghost-gluon vertex. Notice that we have set it up with respect to the antighost leg. (b) Diagrams included in the skeleton expansion of the ghost-gluon kernel that we will consider in our analysis.

quantity, which controls the dynamics of this SDE, is the four-point ghost-gluon kernel.

For the ensuing analysis, we will carry out the following main simplifications:

(i) The ghost-gluon kernel will be replaced by its one-loop dressed approximation; specifically, in the corresponding skeleton expansion, we will only include the diagrams appearing in Fig. 4(b). Thus, the approximate version of the SDE that we employ may be cast in the form

$$\Gamma_\nu(-k,-p,k+p) = p_\nu - \frac{i}{2}g^2 C_{\rm A}[(d_1)_\nu - (d_2)_\nu], \tag{3.1}$$

where the diagrams (d_i) are given by

$$(d_1)_\nu = \int_l \Gamma^{[0]}_\rho \Delta^{\rho\sigma}(l)\Gamma_\sigma D(l+k+p)\Gamma_\nu D(l+p),$$
$$(d_2)_\nu = \int_l \Gamma^{[0]}_\rho \Delta^{\rho\sigma}(l)\Gamma_{\nu\sigma\alpha}\Delta^{\alpha\beta}(l-k)\Gamma_\beta D(l+p). \tag{3.2}$$

For notational simplicity, we have suppressed the arguments of the momenta in all vertices; the latter may be easily recovered from the figures and the conventions established in Sec. II. Note also that, in the LG that we use, the gluon propagators appearing in the above expressions assume the completely transverse form of Eq. (2.9).

(ii) The (multiplicative) renormalization of Eq. (3.1) proceeds in the standard way. Specifically, in addition to the renormalization constants and relations given in Eq. (2.13), one must introduce the vertex renormalization for the three-gluon vertex, to be denoted by Z_3, namely, $\Gamma^{\nu\sigma\alpha}_R = Z_3\Gamma^{\nu\sigma\alpha}$, together with the corresponding relation for the coupling renormalization, namely, $g_R = Z_3^{-1}Z_A^{3/2}g$. From this relation, and the last of Eq. (2.13), one has that $Z_3^{-1}Z_A = Z_1^{-1}Z_c$. Then, it is straightforward to show that the contributions of $g^2(d_1)_\nu$ and $g^2(d_1)_\nu$ maintain the same form after renormalization; in fact, this property may be easily established by grouping the integrands in terms of the standard renormalization-group invariant quantities formed by $(g\Gamma_\mu\Delta^{1/2}D)$ and $(g\Gamma^{\nu\sigma\alpha}\Delta^{3/2})$ [44]. Thus, the renormalized version of Eq. (3.1) reads

$$\Gamma^\nu_R(-k,-p,k+p) = Z_1\left\{p_\nu - \frac{i}{2}g_R^2 C_{\rm A}[(d_1)^\nu_R - (d_2)^\nu_R]\right\}, \tag{3.3}$$

where the Z_1 comes from the renormalization of the $\Gamma^\nu(-k,-p,k+p)$ on the lhs.

In what follows we will set $Z_1 = 1$. In the case of the soft ghost configuration, $p = 0$, (which, as we will see, is equivalent to the Taylor kinematics), this choice is imposed by Taylor's theorem; see Eq. (2.6). On the other hand, in the case of the soft gluon configuration, $k = 0$, this choice constitutes an approximation, in the sense that it is motivated by the one-loop finiteness of the (LG) Γ^ν, but is not enforced by an analogous all-order relation.

(iii) In the two aforementioned diagrams, (d_1) and (d_2), we will keep fully dressed propagators but will

replace the fully dressed three-gluon vertex appearing in graph (d_2) by the corresponding tree-level expression, namely,

$$\begin{aligned}\Gamma_{\alpha\mu\nu}(q,r,p) &\to \Gamma^{[0]}_{\alpha\mu\nu}(q,r,p)\\ &= (r-p)_\alpha g_{\mu\nu} + (p-q)_\mu g_{\nu\alpha}\\ &\quad + (q-r)_\nu g_{\alpha\mu}.\end{aligned} \tag{3.4}$$

Furthermore, as will be explained in the corresponding subsections, additional approximations will be imposed on the fully dressed ghost-gluon vertices, depending on the specific details of each kinematic case considered.

B. Soft gluon configuration

We begin with the analysis of the soft gluon configuration, $k = 0$. Evidently, in this case, the ghost-gluon vertex becomes a function of only one momentum, p, and may be described in terms of a single form factor, namely,

$$\Gamma_\nu(0,-p,p) = A(p)p_\nu; \qquad A(p) \equiv A(0,-p,p). \tag{3.5}$$

Therefore, setting $k = 0$ in Eq. (3.1), one is able to isolate the form factor A by means of the projection

$$\begin{aligned}A(p) &= 1 - \frac{i}{2}g^2 C_A[(d_1) - (d_2)];\\ (d_i) &\equiv \frac{p^\nu}{p^2}(d_i)_\nu, \qquad i = 1,2,\end{aligned} \tag{3.6}$$

where the diagrams (d_i) are obtained from those of Eq. (3.2) in the limit $k \to 0$.

The particular kinematic configuration considered here allows one to derive a linear integral equation for the unknown quantity $A(p)$. This becomes possible because, in the limit $k = 0$, the vertex Γ_ν entering in graph (d_1) becomes $\Gamma_\nu(0,-l-p,l+p)$. Thus, the integral (d_1) contains $A(0,-l-p,l+p)$, giving rise to an integral equation for $A(0,-p,p)$. Unfortunately, this favorable set of circumstances does not apply to the remaining ghost-gluon vertices, namely, Γ_σ and Γ_β in graphs (d_1) and (d_2), respectively; their arguments depend on all possible kinematic variables, and the inclusion of the full A would give rise to a (nonlinear) integral equation, too complicated to solve. We therefore approximate all remaining ghost-gluon vertices by their tree-level expressions.

After these comments, and the use of the notation introduced in Eq. (3.6), the diagram (d_1) reads

$$(d_1) = \int_l \frac{(l\cdot p)}{(l+p)^2 p^2}[(l\cdot p)^2 - l^2p^2]D^2(l)\Delta(l+p)A(l). \tag{3.7}$$

To evaluate the contribution of diagram (d_2) notice that, with the gluon propagators in the LG and the bare three-gluon vertex of Eq. (3.4), we have that

$$P^{\rho\sigma}(l)P^{\alpha\beta}(l)\Gamma^{[0]}_{\nu\sigma\alpha}(0,l,-l) = 2l_\nu P^{\rho\beta}(l). \tag{3.8}$$

Applying this result we get

$$(d_2) = 2\int_l \frac{(l\cdot p)}{l^2p^2}[l^2p^2 - (l\cdot p)^2]\Delta^2(l)D(l+p). \tag{3.9}$$

The final answer is obtained by substituting Eqs. (3.7) and (3.9) in Eq. (3.6); it will be written directly in Euclidean space, using the standard transformation rules,

$$\begin{aligned}&-q^2 = q_{\rm E}^2; \qquad \Delta_{\rm E}(q_{\rm E}^2) = -\Delta(-q_{\rm E}^2);\\ &D_{\rm E}(q_{\rm E}^2) = -D(-q_{\rm E}^2); \qquad \int_k = i\int_{k_{\rm E}},\end{aligned} \tag{3.10}$$

and setting

$$\begin{aligned}&l^2 = t; \quad p^2 = x; \quad (l+p)^2 = z; \quad (l\cdot p) = \sqrt{xt}\cos\theta;\\ &\int_{l_E} = \int\frac{d^4l}{(2\pi)^4} = \frac{1}{(2\pi)^3}\int_0^\infty dt\,t\int_0^\pi d\theta\sin^2\theta.\end{aligned} \tag{3.11}$$

Specifically (we suppress the subscript "E"),

$$\begin{aligned}A(x) = 1 &- \frac{\alpha_s C_A}{4\pi^2}\int_0^\infty dt\sqrt{xt}F^2(t)\\ &\times A(t)\int_0^\pi d\theta\sin^4\theta\cos\theta\left[\frac{\Delta(z)}{z}\right]\\ &- \frac{\alpha_s C_A}{2\pi^2}\int_0^\infty dt\sqrt{xt}t\Delta^2(t)\int_0^\pi d\theta\sin^4\theta\cos\theta\left[\frac{F(z)}{z}\right],\end{aligned} \tag{3.12}$$

where we have used $g^2 = 4\pi\alpha_s$ and Eq. (2.12) in order to express the ghost propagators in terms of their dressing functions.

Notice that, in the limit $x = 0$, namely, when the momentum of the ghost leg is also zero, we recover from Eq. (3.12) the tree-level value of the form factor, i.e., $A(0) = 1$.

C. Soft ghost configuration (Taylor kinematics)

We next turn to the case that, according to the discussion presented in Sec. II, is expected to improve the treatment of the ghost SDE. Specifically, in this subsection we will derive an approximate version for A in the soft ghost configuration, to be denoted by

$$\lim_{p\to 0} A(-k,-p,k+p) = A(-k,0,k) \equiv A(k). \tag{3.13}$$

However, before proceeding to this derivation, we will demonstrate that the form factor $A(-k,0,k)$ obtained in the soft ghost configuration is none other than the form factor $A(-k,k,0)$, appearing in the constraint imposed by Taylor's theorem, given by Eq. (2.6). To prove that, let us rewrite the SDE of the ghost propagator, Eq. (2.7), dressing this time the left ghost-gluon vertex instead of the right, i.e.,

$$iD^{-1}(p^2) = ip^2 - g^2 C_A \int_k \Gamma_\mu(k, -k-p, p)\Delta^{\mu\nu}(k) \times \Gamma^{[0]}_\nu(-k, -p, k+p)D(k+p), \quad (3.14)$$

where we have maintained the same momenta flow and Lorentz indices as in Fig. 2. Therefore, using Eq. (2.2) for the Γ_μ in Eq. (3.14), we get (in the LG)

$$F^{-1}(p^2) = 1 + ig^2 C_A \int_k \left[1 - \frac{(k\cdot p)^2}{k^2 p^2}\right] A(k, -k-p, p) \times \Delta(k)D(k+p). \quad (3.15)$$

Evidently, Eqs. (2.11) and (3.15) must furnish an identical result for $F(p^2)$, since the answer cannot depend on which of the two vertices one chooses to dress. Thus, the form factor A is forced to satisfy the equality

$$A(-k, -p, k+p) = A(k, -k-p, p). \quad (3.16)$$

Given that, due to Lorentz invariance, the dependence on the momenta is quadratic, i.e., $A(k^2, p^2, k^2 + p^2 + 2k\cdot p)$, we have immediately that

$$A(k, -k-p, p) = A(-k, k+p, -p). \quad (3.17)$$

So, combining Eqs. (3.16) and (3.17), we arrive at the relation

$$A(-k, -p, k+p) = A(-k, k+p, -p), \quad (3.18)$$

which states that, in the LG, the form factor A of the gluon-ghost vertex is invariant under the exchange of the momenta of the ghost and anti-ghost legs. Notice that this invariance is known to be a consequence of a global $SL(2, R)$ symmetry between the ghost and antighost fields [2], which implies that the LG is a ghost-antighost symmetric gauge fixing choice. Finally, setting $p = 0$ in Eq. (3.18), one obtains the announced result; that is, the A obtained in the soft ghost limit coincides with that of the Taylor kinematics.

As mentioned above, the fact that the kinematic situation considered here is equivalent to the Taylor limit imposes, in a natural way, the value $Z_1 = 1$ for the renormalization constant appearing in Eq. (3.3).

Once the above connection has been established, we return to the derivation of the explicit expression for the form factor A in the soft ghost limit. To that end, we will consider again the diagrams shown in Fig. 4(b), with dressed gluon and ghost propagators, and tree-level values for *all* the interaction vertices. In this configuration, the expressions given in Eq. (3.2) reduce to

$$(d_1)_\nu = p^\rho (k+p)^\sigma \int_l (l+p)_\nu D(l+p)D(l+k+p) \times \Delta(l)P_{\rho\sigma}(l),$$
$$(d_2)_\nu = p^\rho (k+p)^\beta \int_l D(l+p)\Delta(l)\Delta(l-k)P^\sigma_\rho(l) \times P^\alpha_\beta(l-k)\Gamma^{[0]}_{\nu\sigma\alpha}. \quad (3.19)$$

We next outline the general procedure for isolating the $A(-k, 0, k)$ defined in Eq. (3.13). First, we observe that the most general Lorentz decomposition of the diagrams given in Eq. (3.19) is

$$\begin{aligned}(d_i)_\nu = p^\rho (k+p)^\sigma [&f_1 g_{\nu\rho}k_\sigma + f_2 g_{\nu\sigma}k_\rho + f_3 g_{\rho\sigma}k_\nu \\ &+ f_4 g_{\nu\rho}p_\sigma + f_5 g_{\nu\sigma}p_\rho + f_6 g_{\rho\sigma}p_\nu + f_7 p_\nu p_\rho p_\sigma \\ &+ f_8 p_\nu p_\rho k_\sigma + f_9 p_\nu k_\rho p_\sigma + f_{10} p_\nu k_\rho k_\sigma \\ &+ f_{11} k_\nu k_\rho k_\sigma + f_{12} k_\nu k_\rho p_\sigma + f_{13} k_\nu p_\rho k_\sigma \\ &+ f_{14} k_\nu p_\rho p_\sigma], \end{aligned} \quad (3.20)$$

where the corresponding form factors $f_i \equiv f_i(k, p)$ are assumed to be finite in the infrared limit $p \to 0$.

A detailed look at this expansion reveals that only the tensorial structure $g_{\nu\rho}k_\sigma$, accompanying the form factor f_1, can saturate the prefactor $p^\rho(k+p)^\sigma$ and survive when the limit $p \to 0$ is taken. Specifically, we may rewrite Eq. (3.20) as follows:

$$\begin{aligned}(d_i)_\nu &= p^\rho k^\sigma f_1(k, p) g_{\nu\rho}k_\sigma + \mathcal{O}(p)(k+p)_\nu \\ &= k^2 f_1(k, p)p_\nu + \mathcal{O}(p)(k+p)_\nu, \end{aligned} \quad (3.21)$$

where the symbol $\mathcal{O}(p)(k+p)_\nu$ is used to indicate terms that saturate with p_ν or k_ν, but whose form factors are of order $\mathcal{O}(p)$ or higher and will not contribute in the soft ghost configuration. Furthermore, one can perform the Taylor expansion of $f_1(k, p)$ around $p = 0$, namely,

$$\begin{aligned} &f_1(k, p) = f_1(k, 0) + 2(k\cdot p)f_1'(k) + \mathcal{O}(p^2); \\ &f_1'(k) \equiv \frac{\partial}{\partial p^2} f_1(k, p)|_{p=0}. \end{aligned} \quad (3.22)$$

Thus, only the zero-order term of this expansion is relevant for our kinematic configuration, and we obtain finally from Eq. (3.21) the following result:

$$(d_i)_\nu = k^2 f_1(k, 0)p_\nu + \mathcal{O}(p)(k+p)_\nu, \quad (3.23)$$

where the quantity $k^2 f_1(k, 0)$ should be identified as the contribution of the corresponding diagram to $A(k)$, while terms containing the derivatives of f_1 are naturally reassigned to $\mathcal{O}(p)(k+p)_\nu$.

After these observations, it is relatively easy to establish that this generic procedure can be systematically implemented by performing the following steps. (i) Set $p = 0$ from the beginning *inside* the integrals of Eq. (3.19). (ii) Discard all the terms that give rise to structures of the type $\mathcal{O}(p)(k+p)_\nu$. (iii) Determine the contribution of the

diagram that saturates the index of the momentum p^ρ with the metric tensor $g_{\nu\rho}$.

To illustrate in some detail the above procedure, let us focus our attention on the contribution of diagram (d_1), appearing in the first line of Eq. (3.19). Applying step (i), we obtain

$$(d_1)_\nu = p^\rho (k+p)^\sigma \Big\{ \int_l l_\nu D(l) D(l+k) \Delta(l) P_{\rho\sigma}(l) + p_\nu \int_l D(l) D(l+k) \Delta(l) P_{\rho\sigma}(l) \Big\}. \tag{3.24}$$

Now, using criterion (ii), it is easy to recognize that the part of Eq. (3.24) to be retained is given by

$$(d_1)_\nu = -p^\rho I_{\nu\rho}(k), \tag{3.25}$$

where we have defined the integral

$$I_{\nu\rho}(k) = \int_l \frac{(l\cdot k)}{l^2} D(l) D(l+k) \Delta(l) l_\nu l_\rho, \tag{3.26}$$

which may be further decomposed as

$$I_{\nu\rho}(k) = I_1(k^2) g_{\nu\rho} + I_2(k^2) k_\nu k_\rho, \tag{3.27}$$

with

$$\begin{aligned} I_1(k^2) &= \frac{1}{d-1} P^{\nu\rho}(k) I_{\nu\rho}(k); \\ I_2(k^2) &= \frac{1}{k^4(d-1)} (d k^\nu k^\rho - k^2 g^{\nu\rho}) I_{\nu\rho}(k). \end{aligned} \tag{3.28}$$

Thus, using Eqs. (3.27) and (3.28), we obtain from Eq. (3.25) the following result:

$$(d_1)_\nu = -\frac{1}{d-1} p_\nu \int_l \frac{(l\cdot k)}{l^2 k^2} [l^2 k^2 - (l\cdot k)^2] D(l) \times D(l+k) \Delta(l), \tag{3.29}$$

where, according to (iii), we have only written explicitly the contribution that saturates the momentum p^ρ with the metric tensor $g_{\nu\rho}$.

Consider finally the contribution of diagram (d_2). After the shift $l \mapsto -l$, and setting $p = 0$ inside the integral, it becomes

$$(d_2)_\nu = p^\rho (k+p)^\beta \int_l D(l) \Delta(l) \Delta(l+k) P^\sigma_\rho(l) \times P^\alpha_\beta(l+k) \Gamma^{[0]}_{\nu\sigma\alpha}. \tag{3.30}$$

It is then elementary to show that

$$\begin{aligned} &p^\rho (k+p)^\beta P^\sigma_\rho(l) P^\alpha_\beta(l+k) \Gamma^{[0]}_{\nu\sigma\alpha} \\ &= 2p^\rho \frac{l_\nu l_\rho}{l^2(l+k)^2} [l^2 k^2 - (l\cdot k)^2 + (l+k)^2 (l\cdot k)] \\ &\quad + 2p_\nu \frac{[(l\cdot k)^2 - l^2 k^2]}{(l+k)^2} + \mathcal{O}(p)(k+p)_\nu, \end{aligned} \tag{3.31}$$

and, therefore, the part of diagram (d_2) to be saved is

$$(d_2)_\nu = 2p_\nu \int_l \frac{[(l\cdot k)^2 - l^2 k^2]}{(l+k)^2} D(l) \Delta(l) \Delta(l+k) + 2p^\rho Q_{\nu\rho}(k), \tag{3.32}$$

where we have defined the integral

$$Q_{\nu\rho}(k) = \int_l \frac{l_\nu l_\rho}{l^2(l+k)^2} [l^2 k^2 - (l\cdot k)^2 + (l+k)^2 (l\cdot k)] \times D(l) \Delta(l) \Delta(l+k). \tag{3.33}$$

One observes at this point that the first term in Eq. (3.32) is already saturated by p_ν and may be assigned to the form factor $A(k)$ without further considerations. On the other hand, decomposing the integral Eq. (3.33) in the second term as

$$Q_{\nu\rho}(k) = Q_1(k^2) g_{\nu\rho} + Q_2(k^2) k_\nu k_\rho, \tag{3.34}$$

with

$$\begin{aligned} Q_1(k^2) &= \frac{1}{d-1} P^{\nu\rho}(k) Q_{\nu\rho}(k); \\ Q_2(k^2) &= \frac{1}{k^4(d-1)} (d k^\nu k^\rho - k^2 g^{\nu\rho}) Q_{\nu\rho}(k), \end{aligned} \tag{3.35}$$

we obtain from Eq. (3.32) the result

$$(d_2)_\nu = \frac{2}{d-1} p_\nu \int_l \frac{[l^2 k^2 - (l\cdot k)^2]}{l^2 k^2 (l+k)^2} [(l+k)^2 (l\cdot k) - (l\cdot k)^2 - (d-2) l^2 k^2] D(l) \Delta(l) \Delta(l+k), \tag{3.36}$$

where, as before, we have omitted terms of the type $\mathcal{O}(p)(k+p)_\nu$.

Once Eqs. (3.29) and (3.36) have been derived, we will use Eq. (3.6) for projecting out the form factor $A(k)$, as well as Eqs. (3.10) and (3.11), in order to pass to Euclidean space, and subsequently cast the answer in spherical coordinates. Thus, we arrive at the final result:

$$\begin{aligned} A(y) = 1 &- \frac{\alpha_s C_A}{12\pi^2} \int_0^\infty dt \sqrt{yt} F(t) \Delta(t) \\ &\times \int_0^\pi d\theta' \sin^4\theta' \cos\theta' \left[\frac{F(u)}{u}\right] \\ &+ \frac{\alpha_s C_A}{6\pi^2} \int_0^\infty dt F(t) \Delta(t) \int_0^\pi d\theta' \sin^4\theta' \left[\frac{\Delta(u)}{u}\right] \\ &\times [yt(1+\sin^2\theta') - (y+t)\sqrt{yt}\cos\theta']. \end{aligned} \tag{3.37}$$

Notice that, in this case, $y = k^2$, $u = (l+k)^2$, and θ' is the angle between k and l.

IV. NUMERICAL RESULTS

In this section we will carry out a detailed numerical analysis of the equations obtained in the previous sections. Specifically, in the first subsection, we determine $A(0, -p, p)$ by solving the integral equation Eq. (3.12),

using the lattice data of Refs. [11,12] as input for the gluon propagator $\Delta(q)$ and the ghost dressing function $F(q)$ appearing in it. The solution obtained is then compared with the lattice data of Refs. [36,37]. In the second subsection, we solve numerically the coupled system formed by the integral equations of the ghost dressing function (2.16) and of the ghost-gluon vertex in the soft ghost configuration, given by Eq. (3.37). The unique external ingredients used when solving this system are the lattice data for the gluon propagator $\Delta(q)$. The solution obtained for $F(q)$ compares very favorably with the lattice data of Refs. [11,12].

A. Solution for the soft gluon configuration

The integral equation (3.12) is solved through an iterative process, using as input for the gluon propagator and the ghost dressing function the data obtained from the $SU(3)$ quenched simulations of Refs. [11,12], shown in Fig. 5. Note that the lattice data shown have been renormalized at $\mu = 4.3$ GeV, within the MOM scheme. The value of α_s that corresponds to this value of μ may be obtained from the higher-order calculation presented in Ref. [43]; specifically, we have that $\alpha_s(\mu) = 0.22$.

The (violet) dashed line on the left panel of Fig. 6 represents the corresponding solution for $A(0, -p, p)$. We clearly see that $A(0, -p, p)$ develops a sizable peak around the momentum region of 830 MeV. In addition, as had been anticipated in Sec. III B, we confirm numerically that A indeed assumes its tree-level value when $p \to 0$, i.e., $A = 1$. It is also interesting to notice that, in the ultraviolet limit, the form factor gradually approaches its tree-level value.

On the same panel of Fig. 6, we compare our numerical results with the corresponding lattice data obtained in Refs. [36,37] for this particular kinematic configuration. Although the error bars are rather sizable, we clearly see that our solution follows the general structure of the data. In particular, notice that both peaks occur in the same intermediate region of momenta. Evidently, $A(0, -p, p)$ receives a significant nonperturbative correction, deviating considerably from its tree-level value.

In addition, the blue dotted curve, on the left panel of Fig. 6, represents the results for $A(0, -p, p)$ obtained from the approach developed in Ref. [32], based on the infrared completion of expressions derived using operator product expansion (OPE) techniques (see Eq. (19) of Ref. [32], where the result for arbitrary momenta and angles is given). As we can see, both curves display a similar overall behavior, with the peak of the OPE-derived result slightly shifted toward the ultraviolet region.

Turning to the possible relevance of this result for the ghost SDE, let us observe that the gluon momentum k, which has been taken to vanish in this approximation, corresponds precisely to the momentum of integration appearing inside the ghost equation; see Fig. 2. Therefore, strictly speaking, the use of $A(0, -p, p)$ is only justified for a rather limited region of integration, since, for every given value of p, we must have $k \ll p$ or else the approximation breaks down. It is therefore unlikely that the modified kernel will receive appreciable contributions compared to the case where $A(k, -k - p, p) = 1$. This general expectation is fully supported by the detailed numerical analysis presented below. In fact, the result shown in Fig. 6 corresponds to the most "favorable" of situations, where the form of $A(0, -p, p)$ is used regardless of the value of k, i.e., with no restrictions on the range of the d^4k integration.

On the right panel of Fig. 6, we compare the lattice result for $F(p)$ obtained in Refs. [11,12] with the numerical

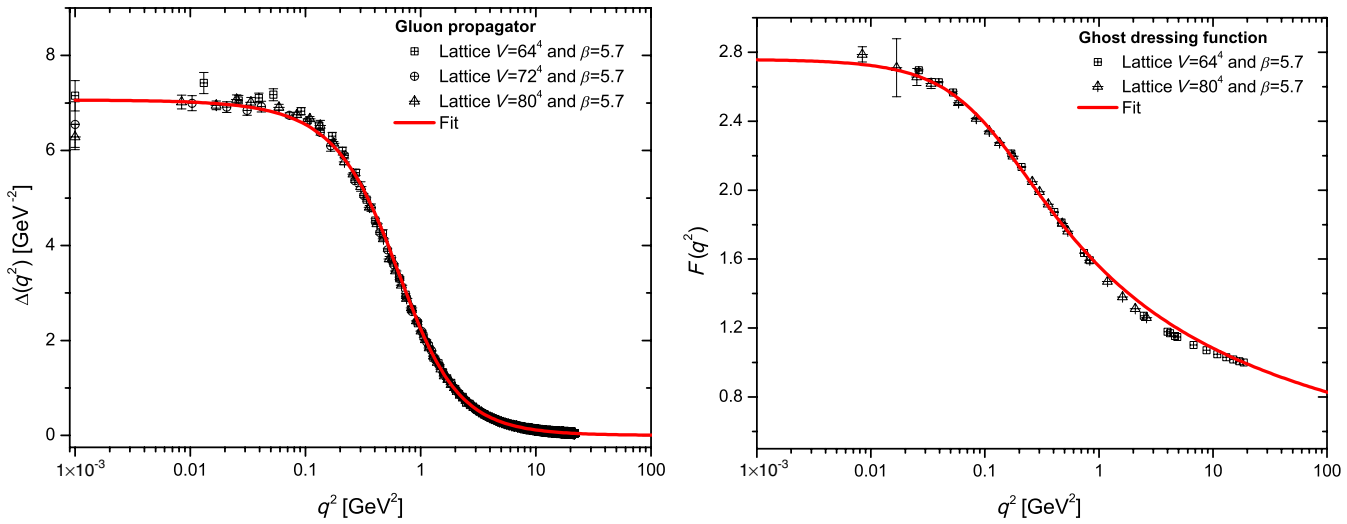

FIG. 5 (color online). Lattice results for the gluon propagator, $\Delta(q)$, (left panel) and ghost dressing, $F(q)$, (right panel) obtained in Refs. [11,12] and renormalized at $\mu = 4.3$ GeV. The (red) continuous curves represent the corresponding fits for the lattice data.

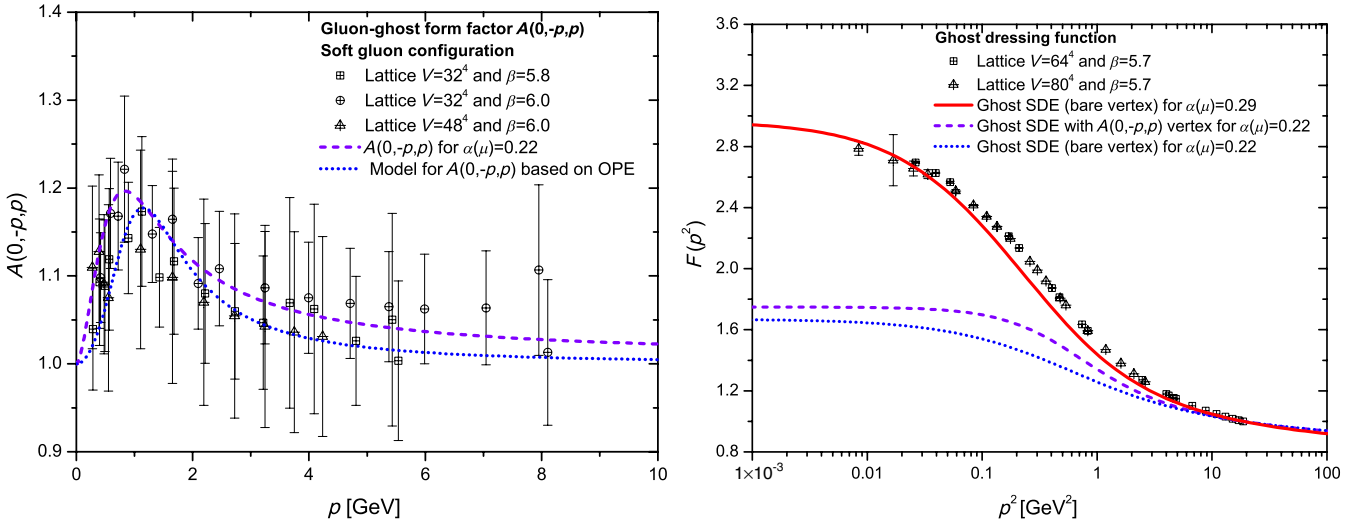

FIG. 6 (color online). *Left panel*: Numerical result for $A(0,-p,p)$, obtained from Eq. (3.12) when $\alpha_s(\mu)=0.22$ (violet dashed line). The (blue) dotted curve represents the prediction of Ref. [32] for the same quantity. *Right panel*: The numerical solution of $F(p)$ compared with the lattice data of Refs. [11,12]. The (red) continuous and the (blue) dotted curves are obtained when the ghost-gluon vertex is approximated by its bare value for $\alpha_s(\mu)=0.29$ and $\alpha_s(\mu)=0.22$, respectively. The (violet) dashed result is obtained using $A(0,-p,p)$ for the ghost-gluon vertex in the ghost SDE with $\alpha_s(\mu)=0.22$.

results obtained with the renormalized ghost SDE of Eq. (2.16) for three different cases. In the first (red continuous curve) and in the second ones (blue dotted curve), we approximate the ghost-gluon form factor by its bare value, i.e., $A(k,-k-p,p)=1$, and we solve the integral equation iteratively for $\alpha_s(\mu)=0.29$ and $\alpha_s(\mu)=0.22$, respectively. The third case, represented by the (violet) dashed line, is obtained when we replace $A(k,-k-p,p)\to A(0,-p,p)$ into Eq. (2.16) and solve it for $\alpha_s(\mu)=0.22$. As mentioned above, $A(0,-p,p)$ is allowed to maintain its deviation from unity throughout the full range of the d^4k integration, and therefore it can be factored outside the integral. The resulting effect is quite unremarkable (less than 5% increase): $F(0)$ increases from $F(0)=1.67$ (bare vertex) to $F(0)=1.75$ (soft gluon vertex) when we use the same value of $\alpha_s(\mu)$.

B. Coupled system: Ghost SDE and ghost-gluon vertex

In this subsection we present the central result of the present article, namely, the modifications induced to the $SU(2)$ and $SU(3)$ ghost dressing function by the inclusion of a nontrivial structure for the corresponding ghost-gluon vertex.

To that end, after passing to the Euclidean space and introducing spherical coordinates, using Eqs. (3.10) and (3.11), we obtain from Eqs. (2.16) and (3.37) the expressions

$$F^{-1}(x)=1-\frac{\alpha_s C_A}{2\pi^2}\int_0^\infty dy\, y\Delta(y)A(y)\times\int_0^\pi d\theta \sin^4\theta\left[\frac{F(z)}{z}-\frac{F(z')}{z'}\right] \quad (4.1)$$

and

$$A(y)=1-\frac{\alpha_s C_A}{12\pi^2}\int_0^\infty dt\sqrt{yt}F(t)\Delta(t)\times\int_0^\pi d\theta' \sin^4\theta'\cos\theta'\left[\frac{F(u)}{u}\right]+\frac{\alpha_s C_A}{6\pi^2}\int_0^\infty dt F(t)\Delta(t)\int_0^\pi d\theta' \sin^4\theta'\left[\frac{\Delta(u)}{u}\right]\times[yt(1+\sin^2\theta')-(y+t)\sqrt{yt}\cos\theta'], \quad (4.2)$$

where now $z=(k+p)^2$, $z'=(k+\mu)^2$, and μ is the renormalization point introduced within the MOM scheme, i.e., by requiring that $F^{-1}(\mu^2)=1$. It is worth mentioning that the ghost SDE of Eq. (4.1) was explored using different truncation schemes in a series of articles [3,15,45–47].

1. $SU(3)$ case

We next solve the above system iteratively, using again the $SU(3)$ lattice data for $\Delta(q)$ and $\alpha_s(\mu)=0.22$ as input. The results for $F(p)$ and $A(-k,0,k)$ are shown in Fig. 7.

On the left panel of Fig. 7, the curve in circles represents the result for $A(-k,0,k)$. Evidently, A develops a peak in the intermediate region of momenta, in a way similar to the case discussed in the previous subsection. In this case the maximum of the peak occurs around 1 GeV, and, once more, in the infrared and ultraviolet limits, $A(-k,0,k)$ assumes its tree-level value. To the best of our knowledge, there are no available $SU(3)$ lattice data for this particular configuration; therefore, the comparison between the $A(-k,0,k)$ obtained with our method and the lattice will be carried out in the next subsection for the case of $SU(2)$.

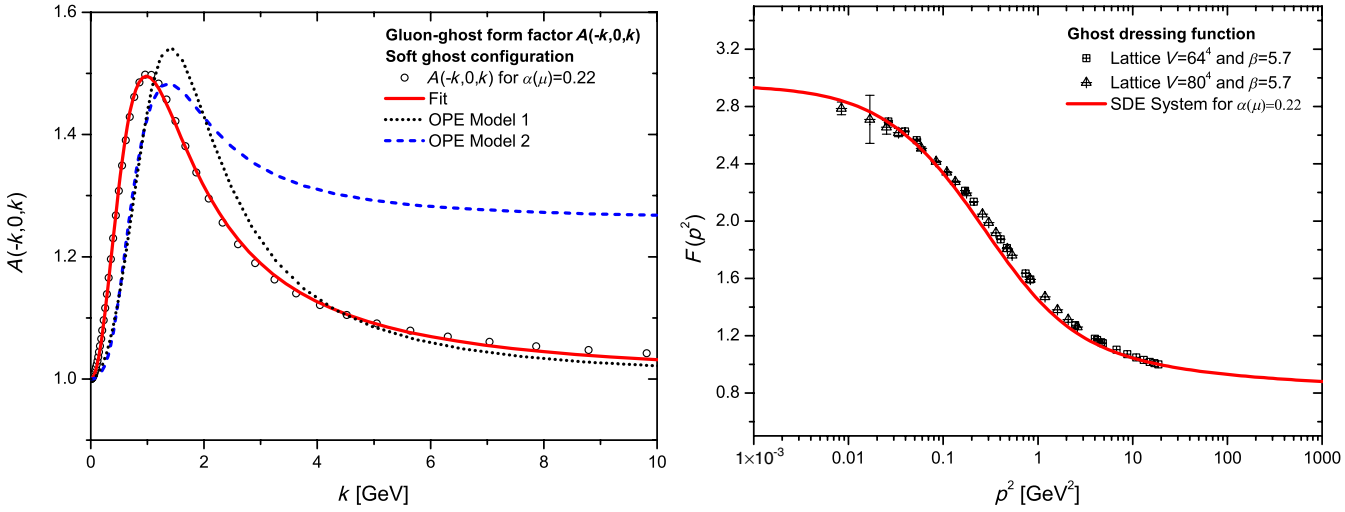

FIG. 7 (color online). *Left panel*: The form factor $A(-k, 0, k)$ (circles) and the fit given by Eq. (4.3) (red continuous line). The (black) dotted and (blue) dashed curves represent the OPE models of Ref. [31]. *Right panel*: The numerical solution of $F(p)$ (red continuous line) compared with the lattice data of Refs. [11,12]. Note that the value of α_s used when solving the system is $\alpha_s(\mu) = 0.22$.

On the same panel, we show a fit for $A(-k, 0, k)$, represented by the (red) continuous curve, whose functional form is given by

$$A(-k, 0, k) = 1 + \frac{ak^2}{[(k^2 + b)^2 + c]} \ln(d + k^2/k_0^2), \qquad (4.3)$$

with the following values for the fitting parameters: $a = 0.68\,\mathrm{GeV}^2$, $b = 0.72\,\mathrm{GeV}^2$, $c = 0.29\ \mathrm{GeV}^4$, $d = 9.62$, and $k_0^2 = 1\ \mathrm{GeV}^2$.

For completeness, on the left panel of Fig. 7, we also compare our results for $A(-k, 0, k)$ with those obtained using two different OPE models, presented in Ref. [31]. The first model is practically that of Ref. [32], but with a new set of parameters, whose values are quoted in Table 3 of Ref. [31]; it is represented by the (black) dotted curve and labeled as model 1 in our legend. Model 2 (blue dashed curve) is a variation of model 1, which, in the deep infrared, adjusts the resulting form factor to its tree-level value. We observe that the three curves have maxima of practically the same height and that all of them are located in the region of 1–1.4 GeV. On the other hand, one notices a slight discrepancy in the UV tails, which ought to be traced back to the different assumptions regarding the finite vertex renormalization that were employed in each case.

On the right panel of Fig. 7, we compare our numerical result for $F(p)$ (red continuous curve) with the corresponding lattice data of Refs. [11,12], observing a rather notable agreement. We emphasize that, contrary to what happens when the bare vertex is used (see Fig. 3), the accuracy achieved here does not rely on the artificial enhancement of the value of the coupling; the latter, as mentioned above, was kept at its standard value predicted from general MOM considerations.

It is important to realize that, although A does not provide a sizable support for ghost SDE in the deep infrared, the contribution that it furnishes in the region of intermediate momenta is sufficient for increasing the saturation point from $F(0) = 1.67$ to $F(0) = 2.95$ (Figs. 3 and 7, respectively). This observation suggests that the ghost SDE is particularly sensitive to the values of its ingredients at momenta around two to three times the QCD mass scale.

2. $SU(2)$ case

We now repeat the analysis of the previous subsection for the $SU(2)$ gauge group. In this case, two separate comparisons may be carried out: $A(-k, 0, k)$ with the lattice data of Ref. [38] and $F(p)$ with those of Ref. [9].

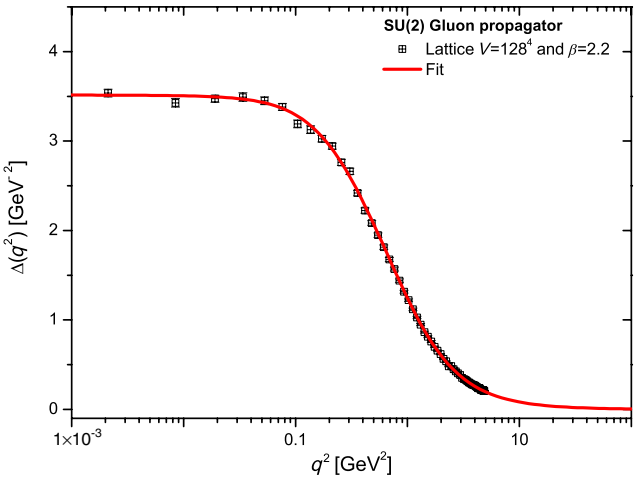

FIG. 8 (color online). The $SU(2)$ lattice data for the gluon propagator, $\Delta(q)$, obtained in Ref. [9] and renormalized at $\mu = 2.2$ GeV. The (red) continuous curve represents the corresponding fit for the lattice data.

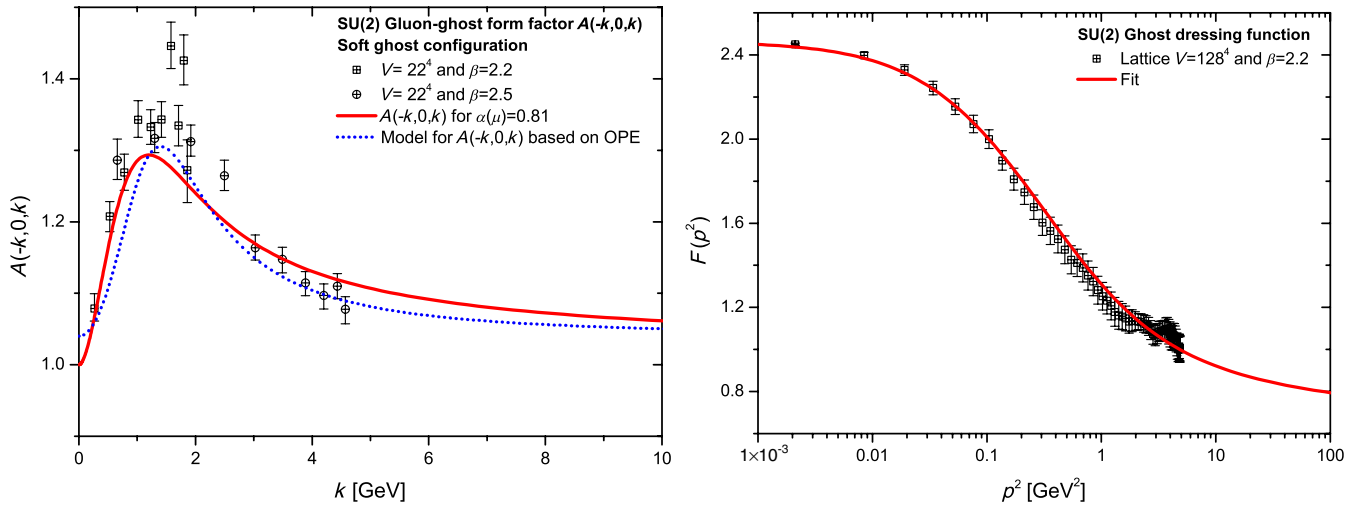

FIG. 9 (color online). *Left panel*: The $SU(2)$ lattice results for $A(-k, 0, k)$ of Ref. [38] (square and circles) and the numerical result for $A(-k, 0, k)$, obtained from the system of Eqs. (4.1) and (4.2) when $\alpha_s(\mu) = 0.81$ (red continuous line). The (blue) dotted line represents the OPE model of Ref. [32]. *Right panel*: Comparison of $F(p)$ (red continuous line), obtained from the system of Eqs. (4.1) and (4.2) with the $SU(2)$ lattice data of Ref. [9].

Specifically, we start by setting $C_A = 2$ in Eqs. (4.1) and (4.2); then we solve the system numerically, using as input the $SU(2)$ data for $\Delta(q)$, presented in Fig. 8 (renormalized at $\mu = 2.2$ GeV), and the value $\alpha_s(\mu) = 0.81$.

On the left panel of Fig. 9, we compare our numerical results for $A(-k, 0, k)$ with the corresponding lattice data obtained in Ref. [38]. Evidently, the solution displays the same qualitative behavior found in the $SU(3)$ analysis, shown in Fig. 7. In particular, for the $SU(2)$ case, the peak is slightly shifted toward the ultraviolet, occurring at around 1.2 GeV. Notice also that our solution follows quite well the general trend of the lattice data but is clearly not on top of them. This deviation, in turn, suggests that the terms discarded from the SDE of the ghost-gluon vertex are indeed small, but not totally negligible.

In addition, on the left panel of Fig. 9, we compare our results for $A(-k, 0, k)$ with those obtained using the aforementioned OPE model of Ref. [32] (blue dotted curve). As we can see, both curves display a similar behavior, with their maximum points located in the region of 1–1.2 GeV. Note that the slight discrepancy at the origin (tree-level result) is due to the finite vertex renormalization employed in Ref. [32]; specifically, $Z_1 = 1.04$, instead of $Z_1 = 1$ that we use here.

Finally, as can be appreciated from the right panel of Fig. 9, our numerical results for $F(p)$ (red continuous curve) are in excellent agreement with the corresponding lattice data of Ref. [9]. As happened in the $SU(3)$ case, the introduction of the nonperturbative correction to the ghost-gluon vertex reduces considerably the value of the gauge coupling needed to reproduce the lattice data. Specifically, when we employ the bare vertex, the lattice result is reproduced for $\alpha_s(\mu) = 0.99$, whereas the value of the coupling used when solving the system of $F(p)$ and $A(-k, 0, k)$ is $\alpha_s(\mu) = 0.81$.

V. CONCLUSIONS

In the present work, we have considered the one-loop dressed approximation of the SDE that governs the evolution of the ghost-gluon vertex. In particular, we have focused on the dynamics of the form factor denoted by A, which is the one that survives in the SDE for ghost dressing function, in the LG. The vertex SDE has been evaluated for two special kinematic configurations, one of them corresponding to the well-known Taylor limit. When coupled to the SDE of the ghost, the contribution of this particular form factor accounts for the missing strength of the associated kernel, allowing one to reproduce the lattice results rather accurately, using the standard value of the gauge coupling constant.

The fact that, despite the truncation implemented on the vertex SDE, we finally obtained a rather good agreement with the lattice, hints to the possibility that the omitted terms are numerically subleading, at least in the case of the special kinematic configurations considered. It might be interesting to pursue this point further. Specifically, in the present analysis, the terms proportional to the second form factor, denoted by B, have been automatically discarded, precisely because they do not contribute to the ghost SDE. However, given that both form factors participate in the fundamental relation of Eq. (2.6), one might consider the possibility of keeping these terms throughout the calculation and then checking explicitly to what extent Eq. (2.6) is satisfied in the present approximation.

Recently, the study of the effects that the dynamical quarks induce on some of the fundamental Green's functions of QCD has received particular attention, both from the point of view of unquenched lattice simulations [48] as well as by means of an SDE-based approach [49]. In particular, lattice simulations reveal that the inclusion of

light active quarks results in a considerable suppression in the deep infrared and intermediate momentum region of the gluon propagator. This characteristic feature has been firmly established also within the SDE framework of Ref. [49]. On the other hand, the unquenched ghost dressing function simulated on the lattice suffers minimal changes from the inclusion of quarks [48]; this property has also been anticipated within the aforementioned SDE analysis [49] as a direct consequence of the fact that, in the case of F, the quark loops enter as "higher-order" effects. In addition, it is well-known that the value of the MOM coupling, $\alpha(\mu)$, increases in the presence of quark loops.

It would be, therefore, interesting, to study the combination of these competing effects systematically, including the vertex equation for A, derived here. In particular, the nonlinear nature of the corresponding integral equations converts this combined analysis into a rather challenging problem. Specifically, the changes induced to the integral equation for A, due to the aforementioned suppression of the gluon propagators entering in it, must be compensated, to a considerable level of accuracy, by the corresponding increase in the coupling constant in order to finally obtain the rather minor change observed in F. We hope to be able to carry out such a study in the near future.

ACKNOWLEDGMENTS

The research of J. P. is supported by the Spanish MEYC under Grant No. FPA2011-23596. The work of A. C. A is supported by the National Council for Scientific and Technological Development-CNPq under the Grant No. 306537/2012-5 and Project No. 473260/2012-3 and by São Paulo Research Foundation-FAPESP through Project No. 2012/15643-1.

[1] C. D. Roberts and A. G. Williams, Prog. Part. Nucl. Phys. **33**, 477 (1994).
[2] R. Alkofer, L. von Smekal, Phys. Rep. **353**, 281 (2001).
[3] C. S. Fischer, J. Phys. G **32**, R253 (2006).
[4] D. Binosi and J. Papavassiliou, Phys. Rep. **479**, 1 (2009).
[5] A. P. Szczepaniak and E. S. Swanson, Phys. Rev. D **65**, 025012 (2001).
[6] A. P. Szczepaniak, Phys. Rev. D **69**, 074031 (2004).
[7] A. C. Aguilar, D. Binosi, and J. Papavassiliou, Phys. Rev. D **78**, 025010 (2008).
[8] A. C. Aguilar and J. Papavassiliou, Phys. Rev. D **83**, 014013 (2011).
[9] A. Cucchieri and T. Mendes, Proc. Sci., LAT2007 (2007) 297; Phys. Rev. Lett. **100**, 241601 (2008); Phys. Rev. D **81**, 016005 (2010); Proc. Sci., LATTICE2010 (2010) 280.
[10] P. O. Bowman, U. M. Heller, D. B. Leinweber, M. B. Parappilly, A. Sternbeck, L. von Smekal, A. G. Williams, and J.-b. Zhang, Phys. Rev. D **76**, 094505 (2007).
[11] I. L. Bogolubsky, E. M. Ilgenfritz, M. Muller-Preussker, and A. Sternbeck, Proc. Sci., LATTICE2007 (2007) 290.
[12] I. L. Bogolubsky, E. M. Ilgenfritz, M. Muller-Preussker, and A. Sternbeck, Phys. Lett. B **676**, 69 (2009).
[13] O. Oliveira and P. J. Silva, Phys. Rev. D **79**, 031501 (2009).
[14] O. Oliveira and P. J. Silva, Proc. Sci., LAT2009 (2009) 226; Phys. Rev. D **86**, 114513 (2012).
[15] M. R. Pennington and D. J. Wilson, Phys. Rev. D **84**, 119901 (2011).
[16] A. Bashir, L. Chang, I. C. Cloet, B. El-Bennich, Y.-X. Liu, C. D. Roberts, and P. C. Tandy, Commun. Theor. Phys. **58**, 79 (2012).
[17] P. Boucaud, J.-P. Leroy, A. L. Yaouanc, J. Micheli, O. Pene, and J. Rodriguez-Quintero, J. High Energy Phys. 06 (2008) 012.
[18] T. Kugo and I. Ojima, Prog. Theor. Phys. Suppl. **66**, 1 (1979).
[19] T. Kugo, arXiv:hep-th/9511033.
[20] P. Watson and R. Alkofer, Phys. Rev. Lett. **86**, 5239 (2001).
[21] K.-I. Kondo, Phys. Rev. D **84**, 061702 (2011).
[22] D. Dudal, J. A. Gracey, S. P. Sorella, N. Vandersickel, and H. Verschelde, Phys. Rev. D **78**, 065047 (2008).
[23] D. B. Leinweber *et al.* (UKQCD Collaboration), Phys. Rev. D **58**, 031501 (1998).
[24] T. Iritani, H. Suganuma, and H. Iida, Phys. Rev. D **80**, 114505 (2009).
[25] O. Oliveira and P. Bicudo, J. Phys. G **38**, 045003 (2011).
[26] J. M. Cornwall, Phys. Rev. D **26**, 1453 (1982).
[27] A. C. Aguilar and J. Papavassiliou, J. High Energy Phys. 12 (2006) 012.
[28] A. C. Aguilar and A. A. Natale, J. High Energy Phys. 08 (2004) 057.
[29] D. Binosi and J. Papavassiliou, Phys. Rev. D **77**, 061702 (R) (2008).
[30] A. C. Aguilar, D. Binosi, and J. Papavassiliou, J. High Energy Phys. 01 (2012) 050.
[31] D. Dudal, O. Oliveira, and J. Rodriguez-Quintero, Phys. Rev. D **86**, 105005 (2012).
[32] P. Boucaud, D. Dudal, J. P. Leroy, O. Pene, and J. Rodriguez-Quintero, J. High Energy Phys. 12 (2011) 018.
[33] A. C. Aguilar, D. Binosi, and J. Papavassiliou, J. High Energy Phys. 07 (2010) 002.
[34] A. Cucchieri, T. Mendes, and A. Mihara, J. High Energy Phys. 12 (2004) 012.
[35] E. M. Ilgenfritz, M. Muller-Preussker, A. Sternbeck, and A. Schiller, arXiv:hep-lat/0601027.
[36] E.-M. Ilgenfritz, M. Muller-Preussker, A. Sternbeck, A. Schiller, and I. L. Bogolubsky, Braz. J. Phys. **37**, 193 (2007).
[37] A. Sternbeck, arXiv:hep-lat/0609016.
[38] A. Cucchieri, A. Maas, and T. Mendes, Phys. Rev. D **77**, 094510 (2008).

[39] W. Schleifenbaum, A. Maas, J. Wambach, and R. Alkofer, Phys. Rev. D **72**, 014017 (2005).
[40] J. Papavassiliou, Nucl. Phys. B, Proc. Suppl. **199**, 44 (2010).
[41] J. C. Taylor, Nucl. Phys. **B33**, 436 (1971).
[42] W. J. Marciano and H. Pagels, Phys. Rep. **36**, 137 (1978).
[43] P. Boucaud, F. De Soto, J. P. Leroy, A. Le Yaouanc, J. Micheli, O. Pene, and J. Rodriguez-Quintero, Phys. Rev. D **79**, 014508 (2009).
[44] A. C. Aguilar, D. Binosi, J. Papavassiliou, and J. Rodriguez-Quintero, Phys. Rev. D **80**, 085018 (2009).
[45] C. S. Fischer, A. Maas, and J. M. Pawlowski, Ann. Phys. (Berlin) **324**, 2408 (2009).
[46] J. Rodriguez-Quintero, AIP Conf. Proc. **1343**, 188 (2011).
[47] J. Rodriguez-Quintero, Phys. Rev. D **83**, 097501 (2011).
[48] A. Ayala, A. Bashir, D. Binosi, M. Cristoforetti, and J. Rodriguez-Quintero, Phys. Rev. D **86**, 074512 (2012).
[49] A. C. Aguilar, D. Binosi, and J. Papavassiliou, Phys. Rev. D **86**, 014032 (2012).